ISSN 1674-1056
http://cpb.iphy.ac.cn
http://iopscience.iop.org/cpb
中国物理 B
Chinese Physics
中国物理
Chinese Physics B

Electronic structures and optical properties of HfO_2-TiO_2 alloys studied by first-principles GGA+*U* approach

Jin-Ping Li(李金平), Song-He Meng(孟松鹤), Cheng Yang(杨程), Han-Tao Lu(陆汉涛), Takami Tohyama(遠山貴巳)
Citation: Chin. Phys. B . 2018, 27(2): 027101. **doi:** 10.1088/1674-1056/27/2/027101

Journal homepage: http://cpb.iphy.ac.cn; http://iopscience.iop.org/cpb

What follows is a list of articles you may be interested in

Optical properties of anatase and rutile TiO_2 studied by GGA+*U*

Jinping Li(李金平), Songhe Meng(孟松鹤), Liyuan Qin(秦丽媛), Hantao Lu(陆汉涛)
Chin. Phys. B . 2017, 26(8): 087101. **doi:** 10.1088/1674-1056/26/8/087101

Visible light absorption of (Fe, C/N) co-doped $NaTaO_3$: DFT+*U*

Peng-Li Tian(田鹏莉), Zhen-Yi Jiang(姜振益), Xiao-Dong Zhang(张小东), Bo Zhou(周波), Ya-Ru Dong(董亚茹), Rui Liu(刘睿)
Chin. Phys. B . 2017, 26(8): 087102. **doi:** 10.1088/1674-1056/26/8/087102

First-principle study of the structural, electronic, and optical properties of SiC nanowires

Wei-Hu Zhang(张威虎), Fu-Chun Zhang(张富春), Wei-Bin Zhang(张伟斌), Shao-Lin Zhang(张绍林), Woochul Yang
Chin. Phys. B . 2017, 26(5): 057103. **doi:** 10.1088/1674-1056/26/5/057103

Stability, electronic structures, and mechanical properties of Fe-Mn-Al system from first-principles calculations

Ya-Hui Liu(刘亚会), Xiao-Yu Chong(种晓宇), Ye-Hua Jiang(蒋业华), Jing Feng(冯晶)
Chin. Phys. B . 2017, 26(3): 037102. **doi:** 10.1088/1674-1056/26/3/037102

Structural, electronic, optical, and magnetic properties of Co-doped Cu_2O

I Djabri, T Rezkallah, F Chemam
Chin. Phys. B . 2017, 26(2): 027102. **doi:** 10.1088/1674-1056/26/2/027102

Electronic structures and optical properties of HfO_2–TiO_2 alloys studied by first-principles GGA + U approach*

Jin-Ping Li(李金平)[1,†], Song-He Meng(孟松鹤)[1], Cheng Yang(杨程)[1], Han-Tao Lu(陆汉涛)[2], and Takami Tohyama(遠山貴巳)[3]

[1] *Center for Composite Materials and Structure, Harbin Institute of Technology, Harbin* 150080, *China*
[2] *Center for Interdisciplinary Studies & Key Laboratory for Magnetism and Magnetic Materials of the MoE, Lanzhou University, Lanzhou* 730000, *China*
[3] *Department of Applied Physics, Tokyo University of Science, Tokyo* 125-8585, *Japan*

(Received 29 August 2017; revised manuscript received 5 November 2017; published online 5 January 2018)

The phase diagram of HfO_2–TiO_2 system shows that when Ti content is less than 33.0 mol%, HfO_2–TiO_2 system is monoclinic; when Ti content increases from 33.0 mol% to 52.0 mol%, it is orthorhombic; when Ti content reaches more than 52.0 mol%, it presents rutile phase. So, we choose the three phases of HfO_2–TiO_2 alloys with different Ti content values. The electronic structures and optical properties of monoclinic, orthorhombic and rutile phases of HfO_2–TiO_2 alloys are obtained by the first-principles generalized gradient approximation (GGA) + U approach, and the effects of Ti content and crystal structure on the electronic structures and optical properties of HfO_2–TiO_2 alloys are investigated. By introducing the Coulomb interactions of 5d orbitals on Hf atom ($U_1^{\rm d}$), those of 3d orbitals on Ti atom ($U_2^{\rm d}$), and those of 2p orbitals on O atom ($U^{\rm p}$) simultaneously, we can improve the calculation values of the band gaps, where $U_1^{\rm d}$, $U_2^{\rm d}$, and $U^{\rm p}$ values are 8.0 eV, 7.0 eV, and 6.0 eV for both the monoclinic phase and orthorhombic phase, and 8.0 eV, 7.0 eV, and 3.5 eV for the rutile phase. The electronic structures and optical properties of the HfO_2–TiO_2 alloys calculated by GGA + $U_1^{\rm d}$ ($U_1^{\rm d}$ = 8.0 eV) + $U_2^{\rm d}$ ($U_2^{\rm d}$ = 7.0 eV) + $U^{\rm p}$ ($U^{\rm p}$ = 6.0 eV or 3.5 eV) are compared with available experimental results.

Keywords: HfO_2–TiO_2 alloys, GGA + U, electronic structure, optical properties

PACS: 71.15.–m, 71.15.Mb, 78.20.Ci, 78.20.Fm **DOI:** 10.1088/1674-1056/27/2/027101

1. Introduction

Among all candidate materials for the gate insulators of metal oxide semiconductor field effect transistors and the capacitor dielectrics of dynamic random access memories, HfO_2 and TiO_2 are promising candidates due to their properties.[1] The phase diagram, cell parameters and geometry structure for HfO_2–TiO_2 system have been studied. The main phase of HfO_2–TiO_2 is monoclinic (denoted as "m"), monoclinic + orthorhombic (denoted as "o"), orthorhombic, and orthorhombic + rutile (denoted as "r"), when TiO_2 content values are less than 5%, 5%∼33%, 33∼52%, and 52∼100%, respectively.[2–5] For example, $HfTiO_4$ (i.e., $Hf_{0.5}Ti_{0.5}O_2$) has a columbite-type (α-PbO_2) structure with two formula units per unit cell, with orthorhombic symmetry, space group pb/cn, with the Hf and Ti atoms randomly distributed on the octahedral site of the α-PbO_2 structure.[6,7]

The phase structure and optical properties of HfO_2–TiO_2 films are determined by preparation process and Ti content. Nanolaminate HfO_2–TiO_2 films are grown by reactive sputter deposition on unheated fused SiO_2, sequentially annealed at 573 K to 973 K. A nanocrystalline structure of orthorhombic $HfTiO_4$ adjacent to an interface followed by monoclinic $Hf_xTi_{1-x}O_2$ was identified.[8] $Hf_xTi_{1-x}O_2$ films on silicon substrates were prepared by the atomic layer deposition. As-deposited $Hf_xTi_{1-x}O_2$ films remained amorphous after annealing up to about 1000 °C in N_2 for 5 min.[1] Hafnium titanate films were deposited in a large Hf–Ti compositional range by atomic layer deposition. The o-$HfTiO_4$ diffraction lines in the samples (30%–64% Hf) annealed at 850 °C have been observed. For an Hf content value higher than 82%, an m-HfO_2-like structure was reported.[9] The x-ray diffraction of a 1:1 mixture of HfO_2 and TiO_2, prepared by the alkoxy hydrolysis technique and heating to ∼ 750 °C, indicated that the material is mainly composed of 95% o-HfTiO.[4] The Ti addition stabilized the amorphous phase of HfO_2. After high-temperature annealing, the films transformed from an amorphous into a polycrystalline phase. The o-Hf–Ti–O peaks were detected in polycrystalline films containing 33 mol% or higher Ti content. As Ti content decreased, m-HfO_2 became the predominant microstructure.[10]

As far as we know, there is no paper studying electronic structure and optical properties of HfO_2–TiO_2 alloys by theoretical calculation based on density function theory, and there are very few studies on electronic structures and optical properties of HfO_2–TiO_2 alloys experimentally.[11] Thus, it is essential to investigate the electron structures of HfO_2–TiO_2 alloys with different phases and Ti content values and clarify the difference in optical property among different structures with

*Project supported by the National Natural Science Foundation of China (Grant Nos. 11672087, 11502058, and 11402252).
†Corresponding author. E-mail: lijinping@hit.edu.cn
© 2018 Chinese Physical Society and IOP Publishing Ltd

variable Ti content from the first-principles calculations.

In this paper we use the GGA scheme and GGA+U scheme formulated by Loschen *et al.*[12] to calculate the lattice parameters, band structures and optical properties of m-, o- and r-$HfTiO_4$ alloys. After introducing the on-side Coulomb interactions of 5d orbitals on Hf atom ($U_1^{\rm d}$), those of 3d orbitals on Ti atom ($U_2^{\rm d}$), and those of 2p orbitals on O atom ($U^{\rm p}$), we can improve the theoretical value of the band gap. By comparing the band gap value with the experimental results of m-HfO_2[13] and r-TiO_2,[14] we obtain the optimal values of $U_1^{\rm d}$, $U_2^{\rm d}$, and $U^{\rm p}$. The electronic structures and optical properties of HfO_2–TiO_2 alloys obtained by GGA+$U_1^{\rm d}+U_2^{\rm d}+U^{\rm p}$ approach are compared with the available experimental results. Finally, we discuss the effects of Ti content and crystal structure on the electronic structures and optical properties of HfO_2–TiO_2 alloys, and give the useful conclusions.

2. Computational method

The first-principles calculations are performed with plane-wave ultrasoft pseudopotential by the GGA with Perdew–Burke–Ernzerhof (PBE) functional and GGA+U approach as implemented in the CASTEP code (Cambridge Sequential Total Energy Package).[15] The ionic cores are represented by ultrasoft pseudopotentials for Hf, Ti, and O atoms. For Hf atom, the configuration is $[He]4f^{14}5d^26s^2$, where the $5d^2$ and $6s^2$ electrons are explicitly treated as valence electrons. For Ti atom, the configuration is $[Ar]3d^24s^2$, where the $3s^2$, $3p^6$, $3d^2$, and $4s^2$ electrons are explicitly treated as valence electrons. For O atom, the configuration is $[He]2s^22p^4$, and $2s^2$ and $2p^4$ treated as valence electrons. The plane-wave cut-off energy is 380 eV, and the Brillouin-zone integration is performed over the $6\times6\times6$ grid sizes by using the Monkhorst–Pack method for structure optimization. This set of parameters assures the total energy convergence of 5.0×10^{-6} eV/atom, the maximum force of 0.01 eV/Å, the maximum stress of 0.02 GPa and the maximum displacement of 5.0×10^{-4} Å.

In the following sections, we optimize the geometry structures of HfO_2–TiO_2 alloys by the GGA, and GGA+$U_1^{\rm d}+U_2^{\rm d}+U^{\rm p}$ when introducing $U_1^{\rm d}$ for Hf 5d orbitals, $U_2^{\rm d}$ for Ti 3d orbitals and $U^{\rm p}$ for O 2p orbitals. By comparing the band gap value with the experimental results of m-HfO_2[13] and r-TiO_2,[14] we obtain the optimal values of $U_1^{\rm d}$, $U_2^{\rm d}$, and $U^{\rm p}$. The resulting electronic structures and optical properties of HfO_2–TiO_2 alloys with different phases and Ti content values obtained by GGA, without U or $U_1^{\rm d}+U_2^{\rm d}+U^{\rm p}$ are presented. Comparison with available experimental data of HfO_2–TiO_2 alloys is also made.

Finally, we calculate electronic structures and optical properties of m-$Hf_{1-x}Ti_xO_2$ ($x=0$ mol%$\sim$50 mol%), o-$Hf_{1-x}Ti_xO_2$ ($x=12.5$ mol%$\sim$ 87.5 mol%), and r-$Hf_{1-x}Ti_xO_2$ ($x=50$ mol%$\sim$ 100 mol%), and study the effects of different phases and Ti content values on the electronic structures and optical properties of HfO_2–TiO_2 alloys. We analyze the change trend and give some reasonable explanations.

3. Results and discussion

3.1. Theoretical results of m-$HfTiO_4$ alloys obtained by GGA+U

The space group of m-$HfTiO_4$ alloy is $p21/c$ and the local symmetry is $C2h$-5. Moreover, m-$HfTiO_4$ alloy is fully characterized by lattice constants a, b, c, and β. In order to check the applicability and accuracy of the ultrasoft pseudopotential, the GGA calculation of the perfect bulk m-$HfTiO_4$ alloy is carried out to determine an optimized a, b, c, and β. The resulting $a=0.507$ nm, $b=0.5174$ nm, $c=0.5337$ nm, and $\beta=99.1^\circ$ are in good agreement with the experimental value, $a=0.5078$ nm, $b=0.5134$ nm, $c=0.5271$ nm, and $\beta=99.2^\circ$.[3]

From the band structure along high-symmetry points in the Brillouin zone, an indirect band gap is observed, and the band gap value $E_{\rm g}$ is about 2.66 eV by GGA. The resulting band gap of m-$HfTiO_4$ alloy obtained by GGA+$U_1^{\rm d}$ ($U_1^{\rm d}=8.0$ eV)+$U_2^{\rm d}$ ($U_2^{\rm d}=7.0$ eV)+$U^{\rm p}$ ($U^{\rm p}=6.0$ eV) approach is 3.35 eV, where $a=0.5211$ nm, $b=0.5025$ nm, $c=0.5531$ nm, and $\beta=99.5^\circ$.

Figure 1 shows the imaginary part ε_2 values of dielectric functions and total density of state (DOS) of m-HfO_2–TiO_2 alloys with different Ti content values, obtained by GGA+U. From Fig. 1, it can be seen obviously that the imaginary part of dielectric function in the m-HfO_2–TiO_2 alloy with 50 mol% Ti is too strange and very different from other m-HfO_2–TiO_2 alloys. Thus, we can suppose that the HfO_2–TiO_2 alloy with 50 mol% Ti is the most impossible to exist as monoclinic phase, which is coincident with experimental results.[3,9,10] From Fig. 1(a), except this alloy with 50 mol% Ti, there are two shoulders in the imaginary part of dielectric functions of each of the other m-HfO_2–TiO_2 alloys and the first shoulder is smaller. With the rise of Ti content, the first shoulder increases gradually while the second one seems to have no obvious regularity.

From Fig. 1(b), total DOS of valence bonds in m-HfO_2–TiO_2 alloys has less changes with Ti content. But they are very different in the conduction bonds of m-HfO_2–TiO_2. Also there are two shoulders in each of the conduction bonds of m- HfO_2–TiO_2 alloys, and total DOS of the m- HfO_2–TiO_2 with 50 mol% Ti is very strange to others, which is similar to the imaginary part of dielectric function (shown in Fig. 1(a)). With the rise of Ti content, the first shoulder increases and the second one decreases gradually.

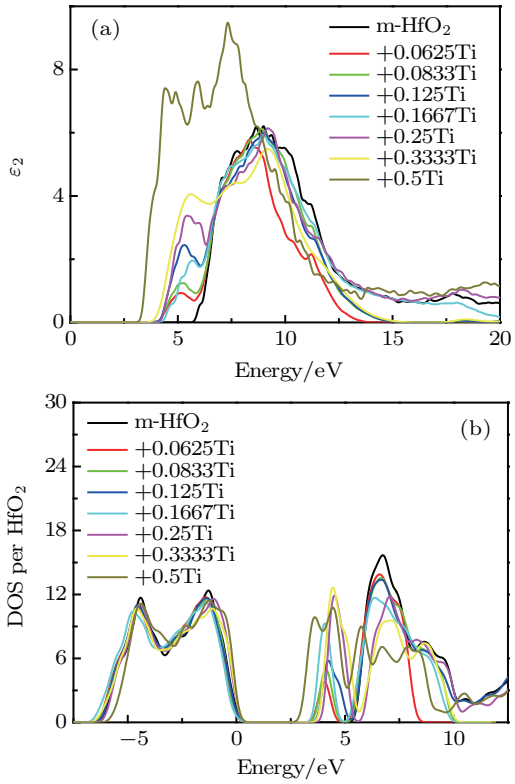


Fig. 1. (color online) (a) Imaginary part values of dielectric functions and (b) total density of state (DOS) in m-HfO_2–TiO_2 alloys with different Ti content values, obtained by GGA+U.

The total DOS curves in the conduction bands shift leftwards. Namely, the position energies of the two shoulders decrease. It is easy to understand the reason why the ε_2 value and total DOS in m- HfO_2–TiO_2 alloys vary. The total DOS in conduction bands near Fermi surface is mainly composed of Hf 5d state and Ti 3d state, where the first shoulder and the second shoulder correspond to Ti 3d state and Hf 5d state, respectively. It is well known that the energies of positions of Ti 3d state and Hf 5d state are about 3.0 eV[14] and 5.8 eV,[13] respectively, similar to the energies of positions of the two shoulders in total DOS of conduction bands near Fermi surface. The resulting denser available state (for Hf 5d state) in the conduction bands has wiped out the higher shoulder, while the thinner states (for Ti 3d state) have wiped out the lower shoulder in the imaginary part of dielectric function, respectively.

3.2. Theoretical results of o-$HfTiO_4$ alloy obtained by GGA+U

The space group of o-$HfTiO_4$ alloy is pb/cn and the local symmetry is D2h-14. Moreover, o-$HfTiO_4$ alloy is fully characterized by lattice constants a, b, and c. In order to check the applicability and accuracy of the ultrasoft pseudopotential, the GGA calculation of the perfect bulk o-$HfTiO_4$ alloy is carried out to determine an optimized a, b, and c. The resulting $a = 0.5073$ nm, $b = 0.5777$ nm, and $c = 0.5242$ nm are in good agreement with the experimental values, $a = 0.4756$ nm, $b = 0.5563$ nm, and $c = 0.5047$ nm.[3]

From the band structure along the high-symmetry points in the Brillouin zone, an indirect band gap is observed, and the band gap value E_g is about 2.99 eV from the GGA. The resulting band gap of o-$HfTiO_4$ alloy obtained by GGA+U_1^d ($U_1^d = 8.0$ eV)+U_2^d ($U_2^d = 7.0$ eV)+U^p ($U^p = 6.0$ eV) approach is 4.397 eV, where $a = 0.4957$ nm, $b = 0.5716$ nm, and $c = 0.5269$ nm.

Figure 2 shows the imaginary part of dielectric function and total density of state (DOS) of each of o-HfO_2–TiO_2 alloys with different Ti content values, obtained by GGA+U. In this case of orthorhombic phase, the Ti content varies in a range from 12.5 mol% to 87.5 mol%. Figure 2(a) shows that there are also two shoulders in the imaginary part of dielectric function of each of o-HfO_2–TiO_2 alloys and the energy difference between the two shoulders is much smaller. When Ti content is more than 37.5%, the two shoulders almost merge together. With the rise of Ti content, the first shoulder increases gradually while the second one decreases. Besides, there is a small shoulder near 40 eV, resulting from Ti 3p state. Thus, its height increases with Ti content increasing.

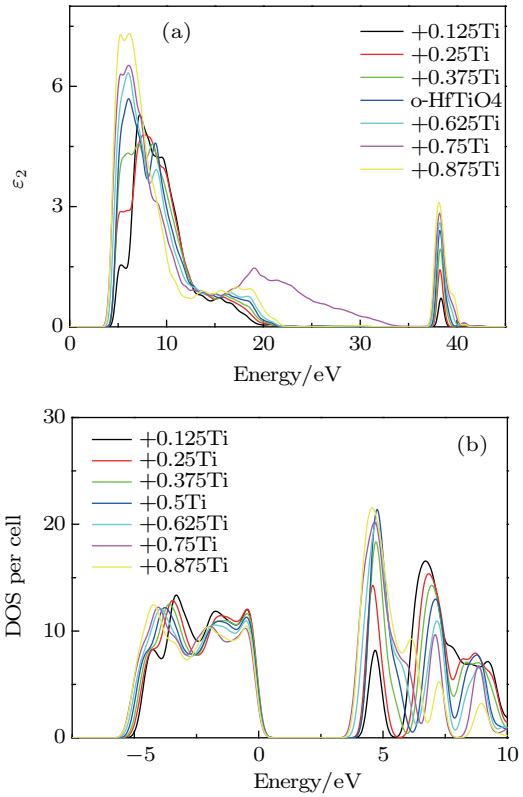


Fig. 2. (color online) (a) Plots of imaginary part of dielectric function and (b) total density of state (DOS) in o-HfO_2–TiO_2 alloys with different Ti content values versus energy, obtained by GGA+U.

Figure 2(b) shows that the total DOS of valence bonds in each of o-HfO_2–TiO_2 alloys with different Ti content values less changes with Ti content. But there is much difference happening to the conduction bonds of o-HfO_2–TiO_2. Also at

energy less than 7.5 eV, there are two shoulders in conduction bond of each of o-HfO_2–TiO_2 alloys, which is similar to the imaginary part of dielectric function (shown in Fig. 2(a)). With the rise of Ti content, the first shoulder increases, while the second decreases regularly.

The total DOS curves in the conduct bands shift leftwards. Namely, the position energies of the two shoulders decrease, which is similar to those in m- HfO_2–TiO_2 alloys. The reason for variations of ε_2 and total DOS in o-HfO_2–TiO_2 alloys is the same as that in m-HfO_2–TiO_2 alloys. By adopting these U values ($U_1^{\rm d} = 8.0$ eV, $U_2^{\rm d} = 7.0$ eV, and $U^{\rm p} = 6.0$ eV), we perform the GGA+U calculation. In the band dispersion, the bottom of the conduction band is located at the G/B point. Since the bottom shift to higher energy with $U^{\rm d}$ accompanied by the reconstruction of the conduction band, the separated DOS at 3.6 eV, 5.7 eV, and 6.7 eV obtained by GGA+U are shown in Fig. 3(a). The conduction band is predominantly constructed by Hf 5d states and by Ti 3d states, while the valence band is by O 2p states as shown in Figs. 3(b)–3(d), respectively. Therefore, the excitation across the gap is from the O 2p states to the Hf 5d states and Ti 3d states.

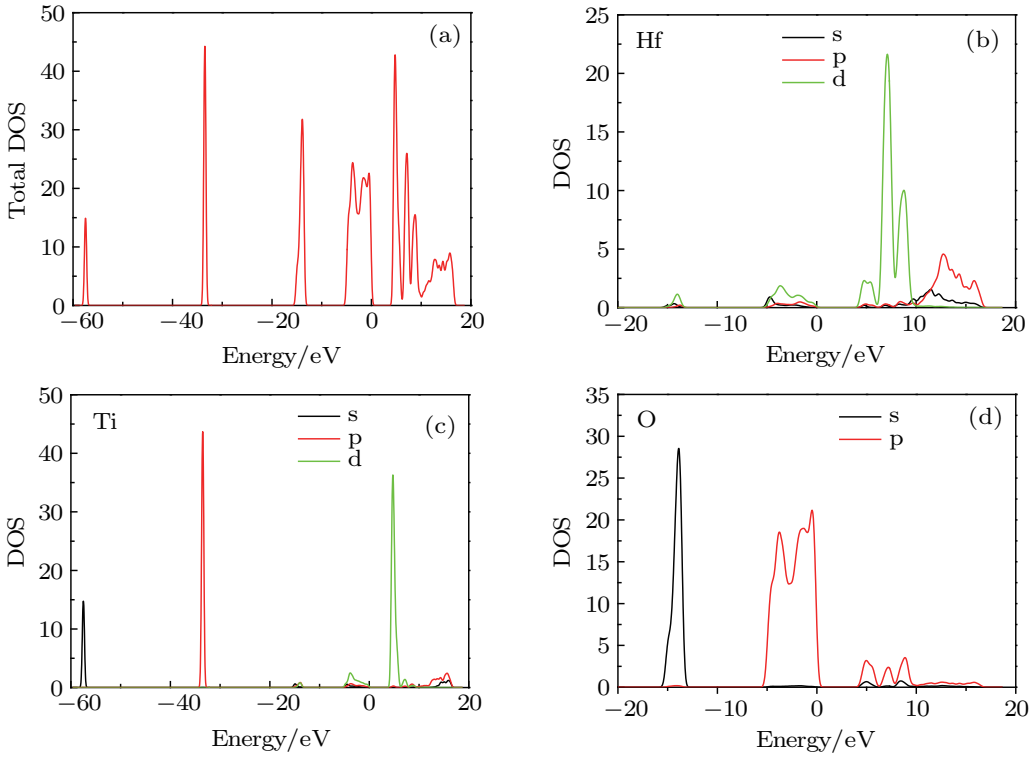


Fig. 3. (color online) Density of states (DOS) of o-HfO_2–TiO_2 calculated by use of GGA+$U^{\rm d}$ ($U^{\rm d} = 8.0$ eV)+$U^{\rm p}$ ($U^{\rm p} = 6.0$ eV). (a) Total DOS, (b) partial DOS of Hf atom, (c) partial DOS of Ti atom, and (d) partial DOS of O atom.

It is well known from crystal field theory[16] that the two peaks in the conduction bands are a result of the ligand field splitting of the Ti 3d and Hf 5d orbitals into two sets of t_{2g} and e_g states. The third shoulder in the Fig. 2(b) may arise from this reason.

A comparison of our results about o-$Hf_{0.875}Ti_{0.125}O_2$ alloy with the experimental results of imaginary part of dielectric function in the $Hf_{0.88}Ti_{0.12}O_2$ film after annealing at high temperature in Ref. [10] is shown in Fig. 4. From Fig. 4 we can see that there are two shoulders, in which the first shoulder is smaller and the second is higher in both experimental and theoretical results. We also find that the magnitudes of ε_2 in our work are different from the experimental ones. The difference may partly come from the fact that the samples of HfO_2–TiO_2 reported in Ref. [10] were mixed with an amount of monoclinic HfO_2. In our calculations, ε_2 of o-HfO_2–TiO_2 also has two shoulders. But the first is higher and the second is lower than the experimental data. It is easy to understand that when o-HfO_2–TiO_2 mixed m-HfO_2, the first shoulder should decrease and the second should increase in the experimental ε_2 results.

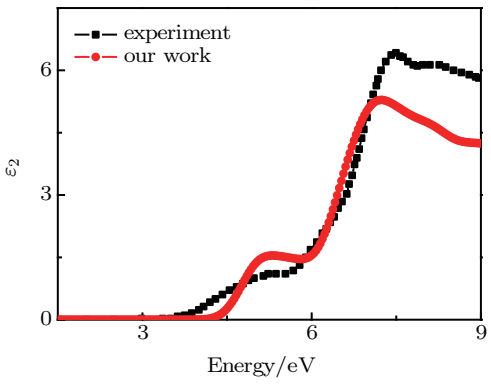


Fig. 4. (color online) Comparison of imaginary part of dielectric function in o-$Hf_{0.875}Ti_{0.125}O_2$ alloy between experimental (in black color) and theoretical results (in red color).

3.3. Theoretical results of r-$HfTiO_4$ alloys obtained by GGA+U

The space group of r-$HfTiO_4$ alloy is $p42/mnm$ and the local symmetry is $D4h$-14. Moreover, r-$HfTiO_4$ alloy is fully characterized by lattice constants a and c. In order to check the applicability and accuracy of the ultrasoft pseudopotential, the GGA calculation of the perfect bulk r-$HfTiO_4$ alloy is carried out to determine an optimized a and c. The results are $a = 0.4856$ nm and $c = 0.3165$ nm, there are no experimental values available to be compared with, and we give the experimental data of cell parameters of rutile TiO_2, $a = 0.4594$ nm and $c = 0.2959$ nm.[17,18]

From the band structure along the high-symmetry points in the Brillouin zone, an indirect band gap is observed, and the band gap value E_g is 2.035 eV from the GGA. The resulting band gap of r-$HfTiO_4$ alloy obtained by GGA+U_1^d ($U_1^d = 8.0$ eV)+U_2^d ($U_2^d = 7.0$ eV)+U^p ($U^p = 3.5$ eV) approach is 3.247 eV, where $a = 0.4869$ nm and $c = 0.3280$ nm.

Figure 5 shows the imaginary part of dielectric function and total density of state (DOS) of each of the r-HfO_2–TiO_2 alloys with different Ti content values, obtained by GGA+U. In this case of rutile phase, the Ti content is varied from 50 mol% to 100 mol%. From Fig. 5(a), there are also three shoulders in the imaginary part of dielectric function of each of the r-HfO_2–TiO_2 alloys and the energy difference between two shoulders on the left is much smaller. With the rise of Ti content, the third shoulder increases gradually. Besides, there is a small shoulder near 40 eV, resulting from Ti 3p state. Thus, with the rise of Ti content, it changes higher and higher.

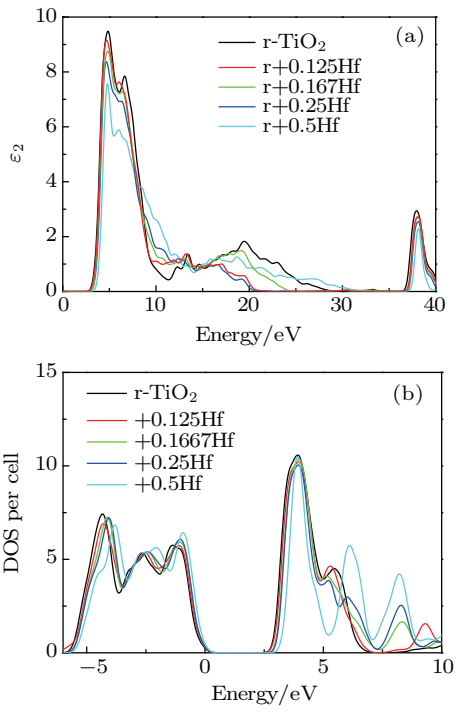


Fig. 5. (color online) Plots of (a) imaginary part of dielectric function and (b) total density of state (DOS) in r-HfO_2–TiO_2 alloys with different Ti content values versus energy, obtained from GGA+U.

From Fig. 5(b), total DOS near Fermi surface in each of the r-HfO_2–TiO_2 alloys less changes with Ti content. Also there are three shoulders in conduction bonds of r-HfO_2–TiO_2 alloy, which is similar to the scenario of imaginary part of dielectric function (shown in Fig. 5(a)). With the rise of Ti content, the first and the second shoulders decrease, and the third shows no regularity. We note that the DOS on the conduction band of the HfO_2–TiO_2 alloy with 50-mol% Ti is too strange, and we suppose that it is impossible to exist as rutile phase.

In Fig. 5(b), the total DOS curves seem unchangeable with the rise of Ti content. Namely, both the position energies and the heights of the shoulders change less. It is easy to understand the reason for the variations of ε_2 and total DOS in r-HfO_2–TiO_2 alloy. In the rutile HfO_2–TiO_2 alloy, except the r- HfO_2–TiO_2 alloy with 50-mol% Ti, the others are composed of the small amount of Hf (varying from 0 mol% to 25 mol%). Thus, the imaginary part of dielectric function and the total DOS are mainly determined by Ti atoms, which is similar to the case for pure rutile TiO_2.

4. Conclusions

From the phase diagram of HfO_2–TiO_2 systems, we choose three phases of HfO_2–TiO_2 alloys with different Ti content values, i.e., monoclinic phase with a Ti content value of less than 50.0 mol%, orthorhombic phase with a Ti content value in a range from 12.5 mol% to 87.5 mol%, and rutile phase with Ti content value more than 50.0 mol%. The electronic structures and optical properties of monoclinic, orthorhombic, and rutile phase of HfO_2–TiO_2 alloys are obtained by the first-principles generalized gradient approximation (GGA)+U approach, and the effects of Ti content and phase on the electronic structure and optical properties of each of the HfO_2–TiO_2 alloys are discussed. By introducing the Coulomb interactions of 5d orbitals on Hf atom (U_1^d), those of 3d orbitals on Ti atom (U_2^d) and those of 2p orbitals on O atom (U^p) simultaneously, we can improve the calculation value of the band gap, where U_1^d, U_2^d, and U^p values are 8.0 eV, 7.0 eV, and 6.0 eV for monoclinic phase, 8.0 eV, 7.0 eV, and 6.0 eV for orthorhombic phase, and 8.0 eV, 7.0 eV, and 3.5 eV for rutile, respectively. The electronic structure and optical properties of the HfO_2–TiO_2 alloy are calculated by GGA+U_1^d ($U_1^d = 8.0$ eV)+U_2^d ($U_2^d = 7.0$ eV)+U^p ($U^p = 6.0$ eV or 3.5 eV) and the results are compared with available experimental data. From the above calculation results, it can be concluded that the HfO_2–TiO_2 alloys with 50-mol% Ti exist only as orthorhombic phase, neither as monoclinic phase nor rutile phase.

References

[1] Qian T, Kueltzo A, Manish S, Jursich G and Takoudis C G 2011 *J. Electrochem. Soc.* **158** G27

[2] Errandonea D, Santamaria-Perez D, Bondarenko T and Khyzhun O 2010 *Mater. Res. Bull.* **45** 1732
[3] Coutures J P and Coutures J 1987 *J. Am. Ceram. Soc.* **70** 383
[4] Mazdiyasni K S and Brown L M 1970 *J. Am. Ceram. Soc.* **53** 585
[5] Yamamoto A, Yamada T, Ikawa H, Fukunaga O, Tanaka K and Marumo F 1991 *Acta Cryst. C* **47** 1588
[6] Seo M, Kim S K, Min Y S and Hwang C S 2011 *J. Mater. Chem.* **21** 18497
[7] Krebs M A and Sr R A C 1988 *J. Mater. Sci. Lett.* **7** 1327
[8] Cisneros-Morales M C and Aita C R 2008 *Appl. Phys. Lett.* **93** 021915
[9] Popovici M, Delabie A, Elshocht S V, Clima S, Pourtois G, Nyns L, Tomida K, Menou N, Opsomer K, Swerts J, Detavernier C, Wouters D, and Kittla J A 2009 *J. Electrochem. Soc.* **156** G145
[10] Triyoso D H, Hegde R I, Zollner S, Ramon M E, Kalpat S, Gregory R, Wang X D, Jiang J, Raymond M, Rai R, Werho D, Roan D, White B E Jr and Tobin P J 2005 *J. Appl. Phys.* **98** 054104
[11] Mazur M, Wojcieszak D, Domaradzki J, Kaczmarek D, Poniedziałek A, and Domanowski P 2015 *Mater. Res. Bull.* **72** 116
[12] Loschen C, Carrasco J, Neyman K M and Illas F 2007 *Phys. Rev. B* **75** 035115
[13] Li J P, Han J C, Meng S H, Lu H T and Tohyama T 2013 *Appl. Phys. Lett.* **103** 071916
[14] Li J P, Meng S H, Qin L Y and Lu H T 2017 *Chin. Phys. B* **26** 087101
[15] Segall M D, Lindan P J D, Probert M J, Pickard C J, Hasnip P J, Clark S J and Payne M C 2002 *J. Phys.: Condens. Matter* **14** 2717
[16] Asahi R, Taga Y, Mannstadt W and Freeman A J 2000 *Phys. Rev. B* **61** 7459
[17] Choi H, Stathatos E and Dionysiou D D 2006 *Appl. Catal. B: Environ.* **63** 60
[18] Cromer D T and Herrington K 1955 *J. Am. Chem. Soc.* **77** 4708